analytical chemistry

Article

pubs.acs.org/ac

Mechanisms of DNA Sensing on Graphene Oxide

Biwu Liu,† Ziyi Sun,† Xu Zhang, and Juewen Liu*

Department of Chemistry, Waterloo Institute for Nanotechnology, University of Waterloo, Waterloo, Ontario, Canada N2L 3G1

Supporting Information

ABSTRACT: Adsorption of a fluorophore-labeled DNA probe by graphene oxide (GO) produces a sensor that gives fluorescence enhancement in the presence of its complementary DNA (cDNA). While many important analytical applications have been demonstrated, it remains unclear how DNA hybridization takes place in the presence of GO, hindering further rational improvement of sensor design. For the first time, we report a set of experimental evidence to reveal a new mechanism involving nonspecific probe displacement followed by hybridization in the solution phase. In addition, we show quantitatively that only a small portion of the added cDNA molecules undergo hybridization while most are adsorbed by GO to play the displacement role. Therefore, it is possible to improve signaling by raising the hybridization efficiency. A key innovation herein is using probes and cDNA with a significant difference in their adsorption energy by GO. This study offers important mechanistic insights into the GO/DNA system. At the same time, it provides simple experimental methods to study the biomolecular reaction dynamics and mechanism on a surface, which may be applied for many other biosensor systems.

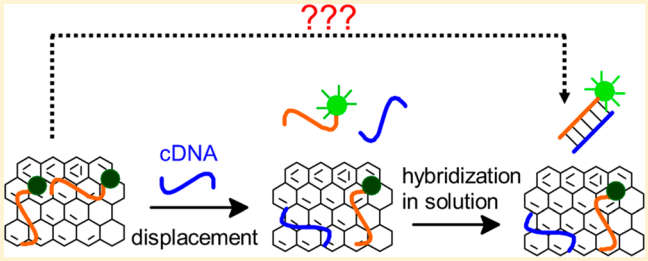

Graphene and graphene oxide (GO) have emerged as an excellent platform for biomolecular adsorption, mediating chemical reactions, and developing biosensors.[1] One particularly interesting and important example is the adsorption of single-stranded (ss) DNA.[2] Even though both are negatively charged, DNA can still be adsorbed by GO in buffers containing a high concentration of salt to screen electrostatic repulsion. The attractive forces between DNA and GO include $\pi-\pi$ stacking, hydrophobic interaction, hydrogen bonding, and van der Waals forces.[3−5] Without a covalent linkage,[6] DNA adsorption is reversible. For example, adsorbed DNA can be desorbed by adding its complementary DNA (cDNA) to form a duplex. Compared to ss-DNA, the affinity between a double-stranded (ds) DNA and GO is much weaker.[7] Since GO is also a fluorescence quencher, fluorophore-labeled DNA and aptamers have been extensively coupled with GO as an analytical tool for detecting nucleic acids,[2,8] metal ions,[9] small molecules,[10−13] proteins,[14] and cells.[15] The GO/DNA sensors have gained extensive interest due to their simplicity in design, high signal-to-background ratio, and great sensitivity, which are critical for developing turn-on fluorescent sensors.[2] Despite these practical applications, it remains unclear how such an analyte-induced desorption reaction takes place at the molecular level. A critical question is whether DNA hybridization can directly occur on the GO surface or in the solution phase. Most previous physical studies only measured adsorption energy with little dynamic information available, thus inadequate to reveal a clear physiochemical picture of the DNA sensing mechanism.[16−18]

If we borrow terms from surface-catalyzed gas-phase reactions, DNA hybridization in the presence of GO can be described by a few possible mechanisms. We herein consider a GO surface preadsorbed with a fluorophore-labeled probe DNA, producing a dark background because of fluorescence quenching by GO. After adding the cDNA (e.g., the target DNA), fluorescence enhancement is observed. If this reaction follows the Langmuir−Hinshelwood mechanism, the cDNA is also adsorbed followed by diffusion on GO. When the cDNA meets a probe DNA, a duplex is formed on the GO surface and then desorbed (Figure 1A). This is a common mechanism for surface-catalyzed gas-phase reactions since both reactants might be activated by the surface to lower the activation energy barrier. Another possibility is the Eley−Rideal mechanism, where the adsorbed probe DNA directly reacts with its cDNA that is dissolved in the solution phase (e.g., the cDNA does not have to be adsorbed at the GO/water interface, Figure 1B) at the GO/water interface. The exact mechanism has not been established with experimental evidence, but most previous work assumed one of the above-mentioned mechanisms.[2] In other words, the general perception on this issue is that at least one DNA is adsorbed by GO during the hybridization reaction.

There are still other possibilities that can also explain the fluorescence enhancement. For example, the added cDNA might compete with the adsorbed probe DNA nonspecifically for surface binding sites. Some of the probe DNA might be displaced by the cDNA into the solution phase to hybridize with the free cDNA (Figure 1C). So far, it has been quite challenging to conclude on a molecular scale mechanism,

Received: June 19, 2013
Accepted: July 23, 2013
Published: July 23, 2013

   dx.doi.org/10.1021/ac401845p | *Anal. Chem.* 2013, 85, 7987−7993

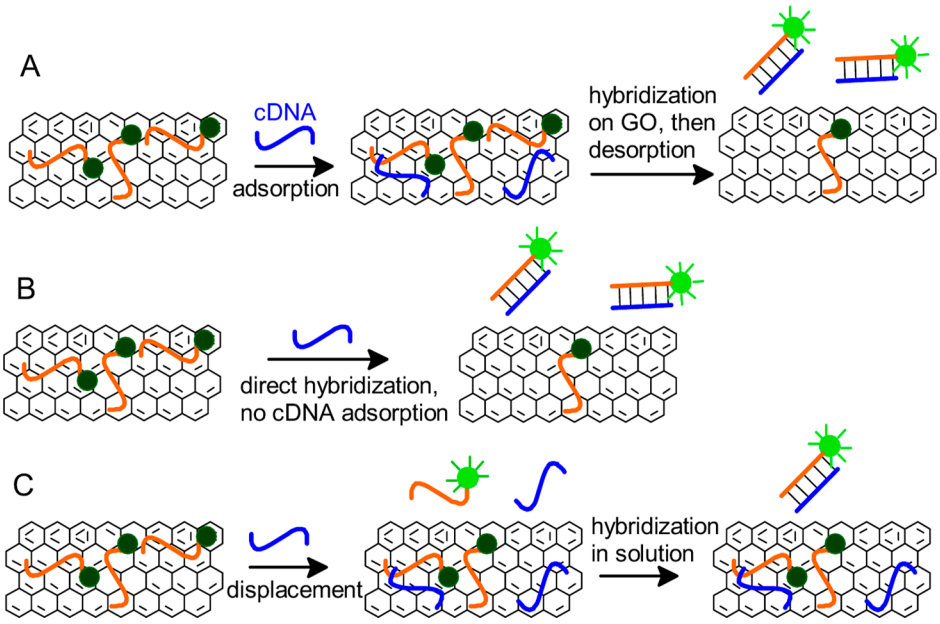

Figure 1. Three possible mechanisms of hybridization between a probe DNA adsorbed by GO and its cDNA (target DNA). The oxygenated groups and defeats on GO are not drawn for clarity of the figures. In all the cases, the probe DNA with a fluorophore label is preadsorbed and the cDNA is added afterward. The tendency of GO adsorbing ds-DNA is lower than that of the adsorption of ss-DNA. (A) Langmuir–Hinshelwood mechanism. (B) Eley–Rideal mechanism. (C) Displacement mechanism.

leading to difficulties toward rational improvement of biosensor design. In addition, considering the extensive research interest on graphene-based materials, understanding its role in biomolecular reactions is crucial for many other applications, including device fabrication, targeted drug delivery, and imaging. We herein report a set of experiments to provide key insights into this important analytical system.

MATERIALS AND METHODS

Chemicals. The dual-labeled DNA samples were from Gene Link Inc. (Hawthorne, NY), and all the other DNAs were from Integrated DNA Technologies (Coralville, IA). See Table 1 for the DNA sequences. The GO sample was purchased from Advanced Chemical Supplier (ACS) Material (Medford, MA).

Table 1. DNA Sequences Used in This Work

DNA name	sequence and modifications (5′ to 3′)	graphic in the paper
FAM-A_{15}	FAM-AAAAAAAAAAAAAAA	Figures 2 and 3
FAM-T_{15}	FAM-TTTTTTTTTTTTTTT	Figures 2 and 3
A_{15}	AAAAAAAAAAAAAAA	Figure 2
T_{15}	TTTTTTTTTTTTTTT	Figure 2
AF-A_{15}	Alexa Fluor 647-AAAAAAAAAAAAAAA	Figure 3
AF-T_{15}	Alexa Fluor 647-TTTTTTTTTTTTTTT	Figure 3
nonstructured probe	FAM-TTCTTTCTTCCCCTTGTTTGTT-TAMRA	Figure 4C
cDNA for nonstructured probe	AACAAACAAGGGGAAGAAAGAA	Figure 4C
hairpin probe	FAM-GCGAGCCAGGTTCTCTTCACAGA TGCGCTCGC-black hole quencher 1	Figure 4D
cDNA for hairpin probe	ACGCATCTGTGAAGAGAACCTGGG	Figure 4D

See Figure S1 (Supporting Information) for a TEM micrograph. The salts and buffers were from Mandel Scientific (Guelph, ON, Canada).

DNA Melting Curves. Carboxyfluorescein (FAM)-labeled DNA (2 μM) was incubated with GO (200 μg/mL) in 10 mM $MgCl_2$ for 1 h followed by three centrifugation (15 000 rpm, 20 min) and washing steps using buffer A (50 mM HEPES, pH 7.6, and 50 mM NaCl). Finally, the complex was dispersed in buffer A with ~50 μg/mL GO in a polymerase chain reaction (PCR) tube. Its fluorescence was monitored as a function of temperature in a real-time PCR thermocycler (CFX-96, Bio-Rad). To measure duplex DNA melting, nonlabeled A_{15} and T_{15} were mixed at 1 μM and annealed in buffer A. A final 5 μM concentration of SYTO-13 dye was added to monitor DNA melting using the thermocycler.

DNA Adsorption/Desorption. The DNA/GO complex was prepared by mixing AF-A_{15} or AF-T_{15} DNA with GO in 2 mM $MgCl_2$, 10 mM HEPES, pH 7.6. The final concentration of GO was 50 μg/mL, and that of DNA was 1 μM. The mixtures were incubated overnight, centrifuged to remove free DNA in the supernatant, and washed with buffer (10 mM HEPES, pH 7.6, 100 mM NaCl). A desorption experiment was carried out with the fluorescence plate reader with two channels (Infinite F200 Pro, Tecan). Each well contained 90 μL of buffer (10 mM HEPES, pH 7.6, 2 mM $MgCl_2$). FAM-labeled A_{15} and T_{15} (final concentration 200 nM) were then added to induce the desorption reaction. Similar procedures were used for desorption of FAM-labeled DNA using nonlabeled DNAs.

Dual-Labeled Probes. Similar procedures were used to study desorption of dual-labeled probes (in Figure 4) from GO, where the adsorbed probe concentration was 5 nM and the cDNA concentration was 200 nM. For the hybridization reaction in solution, 5 nM probe DNA and 200 nM cDNA were mixed in buffer (5 mM HEPES, pH 7.6, with 5 mM $MgCl_2$ and 100 mM NaCl). A lower probe concentration was

dx.doi.org/10.1021/ac401845p | Anal. Chem. 2013, 85, 7987–7993

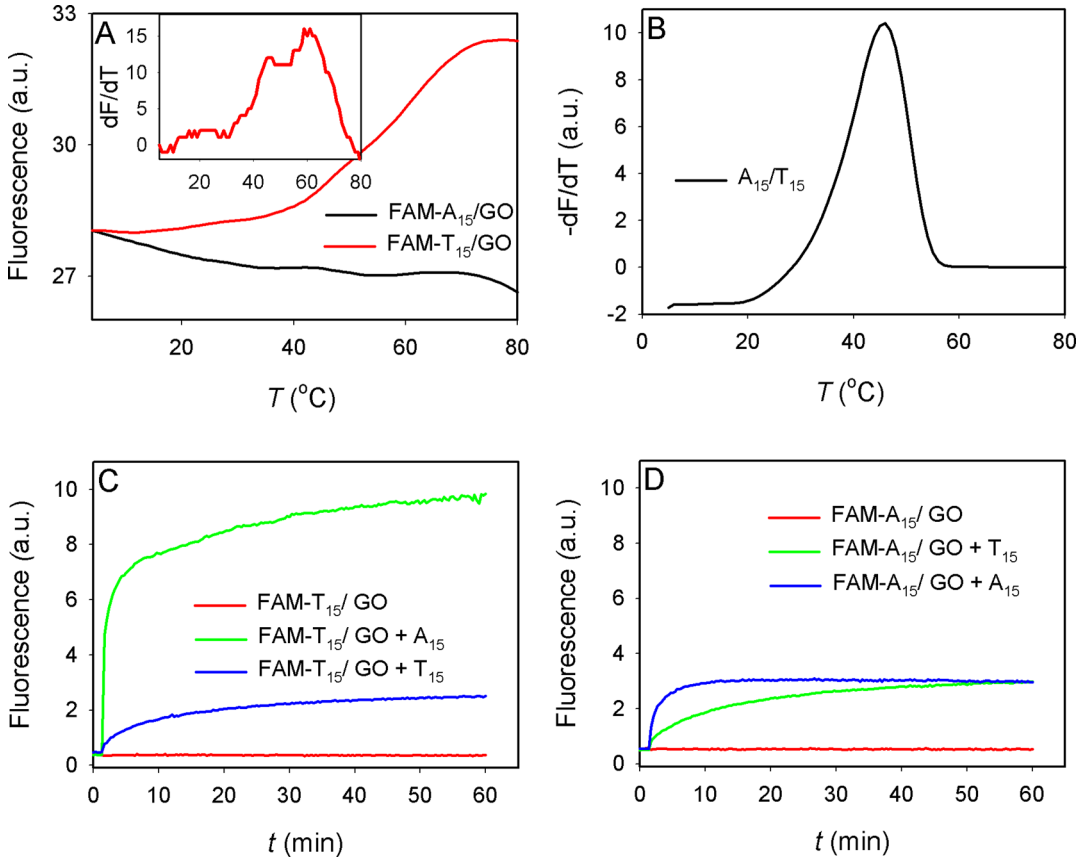

Figure 2. (A) Thermal desorption of FAM-A_{15} and FAM-T_{15} from GO in buffer (50 mM HEPES, pH 7.6, 50 mM NaCl). Inset: first derivative of the FAM-T_{15} desorption profile. (B) A_{15}/T_{15} melting trace (first derivative) in the same buffer. Kinetics of fluorescence enhancement upon adding various DNAs to FAM-T_{15}/GO (C) or to FAM-A_{15}/GO (D). The DNAs were added at 1 min.

used here since we intend to compare the results with those of solution-phase hybridization without GO.

RESULTS AND DISCUSSION

In most previous studies, DNA probes with mixed nucleotide contents were employed for DNA detection. With such sequences, it is likely that both the probe DNA and its cDNA have similar adsorption affinities for the GO surface, thus blurring the hybridization mechanism. We reason that useful insight might be obtained by using DNA homopolymers, which may maximize the difference in the adsorption energy of the DNA probe toward the GO surface relative to that of its cDNA. On the basis of previous studies,[4,19] the purine bases (e.g., A and G) bind to graphene more strongly than the pyrimidines (e.g., T and C). In this study, we chose to test A_{15}/T_{15} (e.g., 15-mer DNA composed of just A or T bases) rather than G_{15}/C_{15}, since poly-G/C can form various secondary structures that may complicate our analysis.

To confirm the order of DNA adsorption affinity, we measured the thermal desorption of 5′-FAM-labeled DNA from GO. The DNA/GO conjugates were exposed to increasing temperatures, and the fluorescence intensity at each temperature was measured, which indicates the amount of desorbed DNA. FAM-A_{15} did not show much desorption, as indicated by the lack of fluorescence increase (Figure 2A, black curve), while FAM-T_{15} showed significant fluorescence enhancement and thus desorption (red curve), confirming its weaker affinity. The melting temperature (T_m, e.g., the maximum of the first derivative) of T_{15} is determined to be 60 °C (inset of Figure 2A). For comparison, we also measured the melting curve of a DNA duplex composed of T_{15}/A_{15} in the absence of GO (Figure 2B), where the T_m was ~44 °C. These experiments indicate that the stability of the T_{15}/A_{15} duplex is slightly lower than that of the T_{15}/GO complex, while A_{15}/GO is the most stable since it fails to dissociate by heating.

It needs to be noted that the surface of GO is highly heterogeneous, containing both highly oxidized domains and crystalline carbon domains.[20,21] DNA adsorbed on the carbon domains is more stable than that on the oxidized domains. This explains the broad desorption profile of FAM-T_{15}/GO in Figure 2A. These melting curves were measured in a low-salt buffer containing just 50 mM NaCl. With a high salt concentration (e.g., 5 mM Mg^{2+}), even FAM-T_{15} failed to desorb (Figure S2, Supporting Information).

After confirming the order of DNA adsorption energy, we next studied DNA-induced desorption. When FAM-T_{15} was used as the preadsorbed probe, adding A_{15} resulted in a large fluorescence increase (Figure 2C, green curve). This is attributed to the formation of the FAM-T_{15}/A_{15} duplex. If a nonlabeled T_{15} was added, a slow and moderate fluorescence increase was observed due to nonspecific displacement of the adsorbed FAM-T_{15} (blue curve) by T_{15}. Without any added DNA, the adsorbed probe DNA was quite stable and the background fluorescence did not change (red curve). This is the typical scenario reported in most DNA detection papers.

Next we employed FAM-A_{15} as the preadsorbed probe. Surprisingly, when T_{15} was added, the fluorescence increase was very slow (Figure 2D, green curve), even slower than the

dx.doi.org/10.1021/ac401845p | Anal. Chem. 2013, 85, 7987−7993

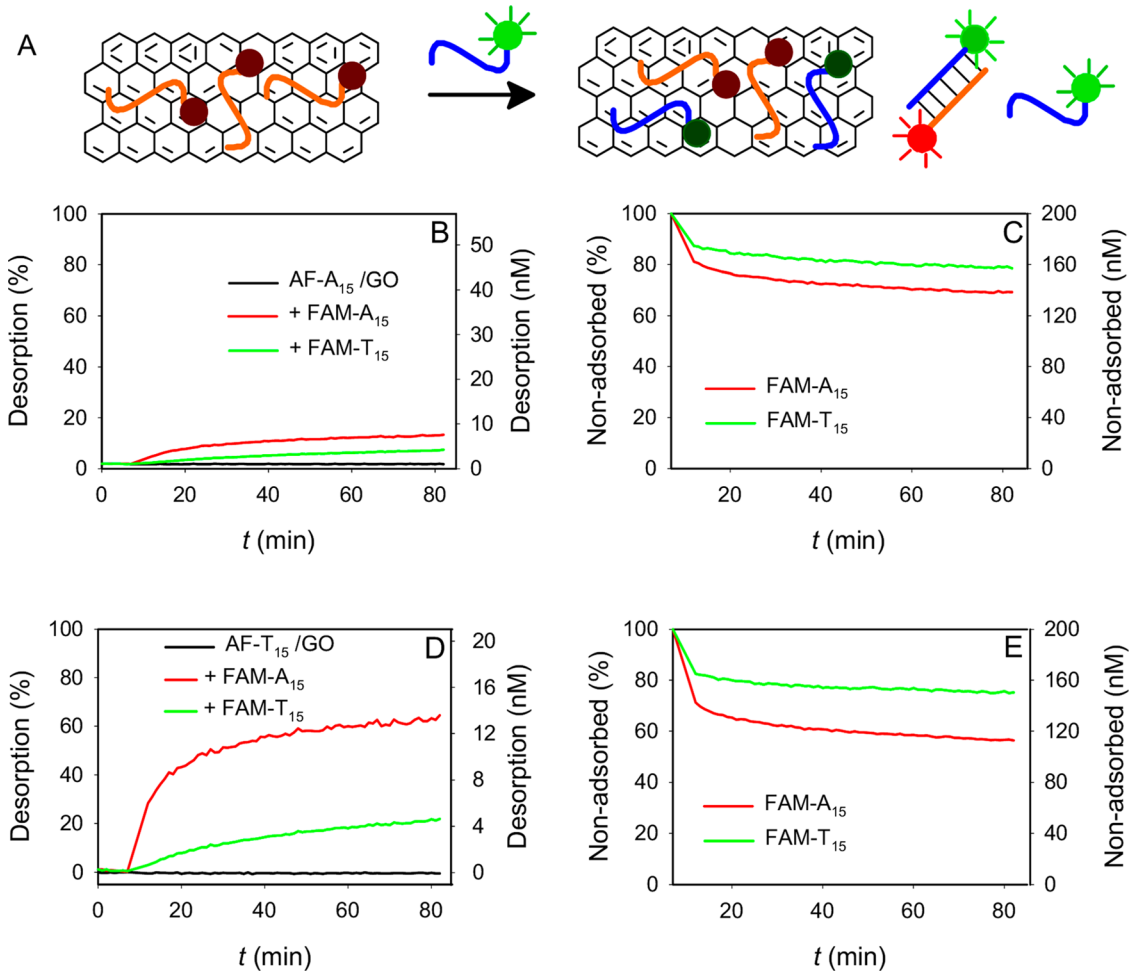

Figure 3. (A) Scheme of quantifying DNA adsorption and desorption using a dual-fluorophore approach. Desorption of AF-A_{15} (B) or AF-T_{15} (D) by FAM-labeled DNA. Adsorption of FAM-labeled DNA in the presence of preadsorbed AF-A_{15} (C) or AF-T_{15} (E) probes. The plots were made to compare both the percentage (the left axis) and absolute concentration (the right axis) of DNA adsorption/desorption.

displacement reaction induced by adding A_{15} (blue curve). This result allows us to rule out the Eley–Rideal mechanism (Figure 1B). If hybridization were taking place on the GO/water interface when FAM-A_{15} was preadsorbed, one would expect more efficient fluorescence enhancement by adding T_{15} than adding A_{15}, because A_{15} cannot hybridize with FAM-A_{15}. Since we observed the opposite, reactions other than hybridization might be the rate-limiting step.

The difference in cDNA-induced desorption between FAM-A_{15} and FAM-T_{15} does not support the Langmuir–Hinshelwood mechanism either (Figure 1A), which contains four steps: adsorption of both DNAs by GO, DNA diffusion on the surface, cDNA/DNA hybridization on GO, and release of the resulting duplex into solution to generate fluorescence. If both DNAs must be adsorbed by GO before hybridization, we expect a similar kinetics regardless of whether FAM-A_{15} or FAM-T_{15} is used as the preadsorbed probe as long as the adsorption kinetics of A_{15} or T_{15} is comparable. To confirm the adsorption kinetics, we respectively monitored the adsorption of FAM-A_{15} and FAM-T_{15} (Figure S3, Supporting Information). Adsorption was finished in ~20 s for both DNAs, much faster than the desorption kinetics. Therefore, the difference in parts C and D of Figure 2 must be due to reactions after the DNA adsorption step. In fact, both mechanisms can be ruled out on the basis of the adsorption energy argument; under our experimental conditions, the DNAs are more stable when they are single-stranded and adsorbed to GO than forming a duplex (Figure 2A,B).

Figure 2D directly points to the importance of nonspecific displacement. Since the mechanisms related to direct DNA hybridization on GO have already been ruled out, we reason that the key step is the displacement of the adsorbed probe DNA by its cDNA. DNA cannot directly hybridize on GO since it is energetically unfavorable to do so. On the other hand, the displacement reaction requires little to no net energy (e.g., in the case of A_{15} displacing FAM-A_{15}) and is driven by the mass action law. In addition, displacement requires lower activation energy than desorption/hybridization since biopolymer displacement on surfaces can often take a concerted mechanism.[22,23] After being displaced, the desorbed probe reacts with the cDNA in solution to form a duplex as schematically shown in Figure 1C. Fluorescence enhancement was due to the unfavorable readsorption of the ds-DNA.

On the basis of the above discussion, the added cDNA or target DNA has two roles: (1) the adsorbed cDNA displaces the probe DNA into solution and (2) the cDNA in solution hybridizes with desorbed probes to prevent its readsorption. Therefore, we can deduce that the target DNA is not utilized efficiently since ideally each target DNA should generate one hybridization event or one desorbed fluorophore. To track the

dx.doi.org/10.1021/ac401845p | Anal. Chem. 2013, 85, 7987–7993

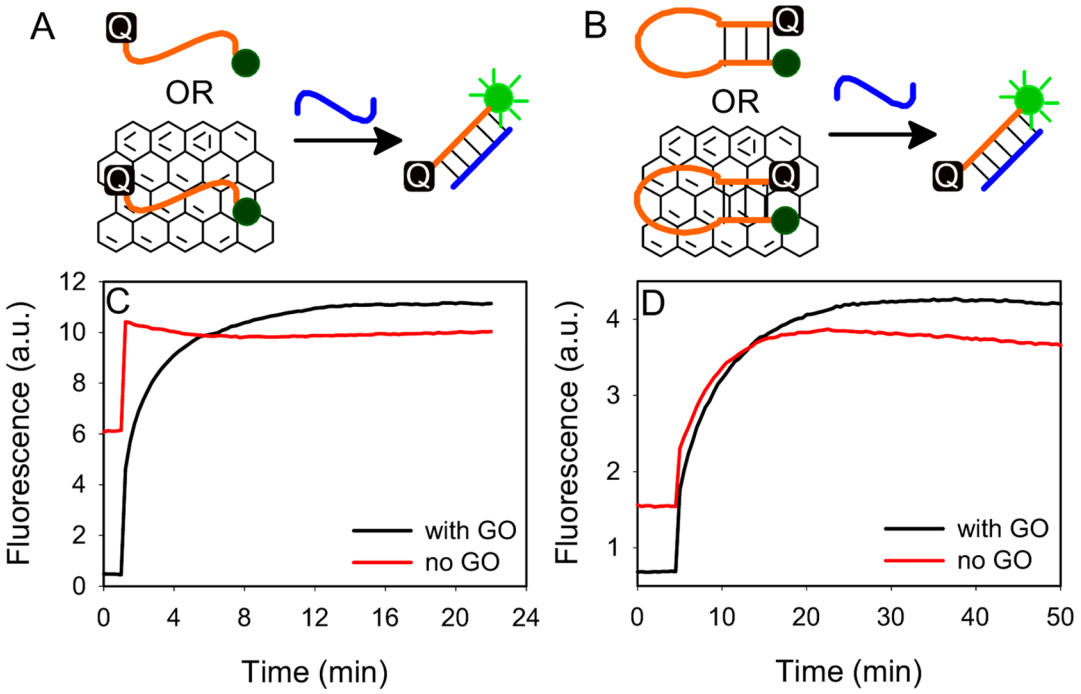

Figure 4. Schematic presentation of hybridization of nonstructured DNA with cDNA (A) or hairpin DNA with cDNA (B) for the free DNA or DNA adsorbed on GO. (C) Hybridization kinetics for the reaction in (A). (D) Hybridization kinetics for the reaction in (B).

partition of cDNA, we employed cDNA labeled with a different fluorophore (Figure 3A). To minimize fluorescence resonance energy transfer (FRET) in the duplex formed between these two DNAs, we chose to use FAM and Alexa Fluor 647 (AF) as labels since they form a poor FRET pair. When AF-A_{15} was preadsorbed as the probe, adding 200 nM FAM-T_{15} resulted in just ~5% or ~3 nM AF-A_{15} desorption (Figure 3B, green line). At the same time, ~40 nM FAM-T_{15} was adsorbed (Figure 3C, green curve). If 200 nM FAM-A_{15} was added, ~8 nM AF-A_{15} was desorbed (Figure 3B, red curve) and 60 nM FAM-A_{15} was adsorbed (Figure 3C, red curve). In both cases, the efficiency of signal generation was quite low. With 200 nM added DNA, only 1.5−4% equivalent of the probe DNA desorbed. We also compared AF-T_{15} desorption induced by FAM-A_{15} and nonlabeled A_{15}, where the kinetics were quite similar, and these labels do not affect the reaction kinetics (Figure S4, Supporting Information). However, we cannot rule out that other fluorophores, especially cationic and hydrophobic ones, might induce a behavior different from that of nonlabeled DNA.

When AF-T_{15} was preadsorbed as the probe, adding 200 nM FAM-A_{15} resulted in ~60% or 14 nM probe desorption (Figure 3D, red line). At the same time, ~80 nM FAM-A_{15} was adsorbed. This is a better signaling condition compared to that in Figure 3B and is analyzed in more detail. We can divide the added 200 nM FAM-A_{15} DNA into three populations. The majority remains in the solution phase as ss-DNA (~106 nM) since the surface has limited capacity. A fraction is in the ds-DNA form (~14 nM) paired with desorbed AF-T_{15}, assuming that the AF-T_{15}/FAM-A_{15} duplex is not readsorbed by GO. Although ds-DNA can also be adsorbed,[7] this is a reasonable assumption here since the surface is already saturated with ss-DNA. The remaining FAM-A_{15} (~80 nM) is adsorbed by the GO surface to displace AF-T_{15}. In the ideal case, all the 200 nM FAM-A_{15} should be used to generate signal by forming a duplex. However, only 14 nM achieved it. In this experiment, we used an excess amount of the FAM-A_{15} to push more probe DNA off the GO surface. If we just consider DNA adsorbed by GO and those formed ds-DNAs, ~14/94 = 15% of the cDNA resulted in the AF-T_{15} probe desorption. In a simple model, to desorb 1 equiv of probe DNA, at least 6−7 equiv of its cDNA needs to be added (sequence dependent). This calculation also supports the displacement mechanism; it takes 6 equiv of cDNA to displace 1 equiv of adsorbed DNA. Despite its low efficiency, such GO-based sensors can still achieve high sensitivity and often detect down to ~1 nM DNA. This is attributed to the extremely low background fluorescence and small background fluctuation. After understanding the reaction mechanism, future work can be geared toward rational improvement of sensor signaling, such as blocking the GO surface after probe adsorption and tuning the probe adsorption energy. We also tested the reaction at lower probe density, and similar results were observed (Figure S5, Supporting Information). Therefore, the displacement mechanism is a general conclusion for this DNA/GO system.

A reaction can take many different routes (e.g., Figure 1), and the one with the lowest activation energy and the fastest rate wins. If DNA hybridization follows the Langmuir−Hinshelwood mechanism, a hidden assumption is that hybridization should be faster on GO (e.g., GO serves as a hybridization catalyst). To study the role of GO, we compared the DNA hybridization rate in the presence and absence of GO. First, a nonstructured DNA probe with terminal fluorophore and quencher labels was employed (Figure 4A). In the absence of GO, hybridization with its cDNA was very fast; the signal was saturated in less than 20 s (Figure 4C, red trace). The amount of fluorescence enhancement was low since the initial distance between the fluorophore and quencher might be quite long already; forming ds-DNA with its cDNA only caused slightly more separation between the fluorophore and quencher. On the other hand, if we first adsorbed the probe DNA by GO, a much slower kinetics was observed, indicating

dx.doi.org/10.1021/ac401845p | *Anal. Chem.* 2013, 85, 7987−7993

that GO is not a catalyst but rather an inhibitor for DNA hybridization in general. This is understandable since DNA binds to GO strongly and this strong interaction has to be disrupted to allow for DNA hybridization.

Next we tested a molecular beacon with a hairpin structure to increase the hybridization activation energy barrier of the free DNA probe (Figure 4B).[24−26] Adsorbing the molecular beacon probes on GO has been shown to suppress the background and enhance selectivity,[8a,27,28] while we used it here for the purpose of mechanistic study. Indeed, the free DNA hairpin hybridization kinetics was much slower (Figure 4D, red curve) compared to that for the nonstructured DNA in Figure 4C. Adsorption of this hairpin to the GO surface resulted in a lower background, and the kinetics of the reaction remains similar. The similar hybridization kinetics with and without GO for the hairpin DNA suggests that the displacement reaction should have a similar or slightly faster rate compared to hairpin hybridization to its cDNA in solution. Otherwise, the fluorescence signaling kinetics should be much slower in the presence of GO. The study of the hairpin probe further supports that GO is not a catalyst for DNA hybridization even when an artificial energy barrier is introduced, thus disproving the Langmuir−Hinshelwood mechanism from another perspective.

CONCLUSIONS

In conclusion, we have developed a set of experiments to probe the surface reaction mechanism of DNA on GO. The key experimental novelty here is to use probe DNA and its cDNA with a large adsorption energy difference on the GO surface. This can be readily achieved by tuning the nucleotide composition. On the basis of our results, the mechanism is probe DNA displacement followed by hybridization in solution, which has not been previously proposed for the GO/DNA system. At its current design, the efficiency of using the cDNA is quite low, and even in the optimal design of using a low-affinity probe and high-affinity cDNA, only ∼15% of the cDNA is used for signal generation. Therefore, there is a lot of room for rational engineering of the interface to improve sensitivity. Similar methods can also be applied to study the reaction mechanism in other bionanosystems.[29]

ASSOCIATED CONTENT

Supporting Information

DNA adsorption/desorption kinetics, additional melting curves, and TEM images. This material is available free of charge via the Internet at http://pubs.acs.org.

AUTHOR INFORMATION

Corresponding Author

*E-mail: liujw@uwaterloo.ca. Phone: 519-888-4567, ext 38919.

Author Contributions

†B.L. and Z.S. contributed equally to this work.

Notes

The authors declare no competing financial interest.

ACKNOWLEDGMENTS

Funding for this work is from the University of Waterloo, the Canadian Foundation for Innovation, the NSERC of Canada, and an Early Researcher Award from the Ontario Ministry of Research and Innovation.

REFERENCES

(1) (a) Geim, A. K.; Novoselov, K. S. *Nat. Mater.* **2007**, *6*, 183−191. (b) Rao, C. N. R.; Sood, A. K.; Subrahmanyam, K. S.; Govindaraj, A. *Angew. Chem., Int. Ed.* **2009**, *48*, 7752−7777. (c) Wang, Y.; Li, Z. H.; Wang, J.; Li, J. H.; Lin, Y. H. *Trends Biotechnol.* **2011**, *29*, 205−212. (d) Kim, J.; Cote, L. J.; Huang, J. *Acc. Chem. Res.* **2012**, *45*, 1356−1364. (e) Chen, D.; Feng, H.; Li, J. *Chem. Rev.* **2012**, *112*, 6027−6053. (f) Loh, K. P.; Bao, Q.; Eda, G.; Chhowalla, M. *Nat. Chem.* **2010**, *2*, 1015−1024. (g) Wang, H.; Yang, R. H.; Yang, L.; Tan, W. H. *ACS Nano* **2009**, *3*, 2451−2460. (h) Guo, S. J.; Dong, S. J. *Chem. Soc. Rev.* **2011**, *40*, 2644−2672.

(2) (a) Lu, C. H.; Yang, H. H.; Zhu, C. L.; Chen, X.; Chen, G. N. *Angew. Chem., Int. Ed.* **2009**, *48*, 4785−4787. (b) He, S. J.; Song, B.; Li, D.; Zhu, C. F.; Qi, W. P.; Wen, Y. Q.; Wang, L. H.; Song, S. P.; Fang, H. P.; Fan, C. H. *Adv. Funct. Mater.* **2010**, *20*, 453−459. (c) Wu, M.; Kempaiah, R.; Huang, P.-J. J.; Maheshwari, V.; Liu, J. *Langmuir* **2011**, *27*, 2731−2738. (d) Guo, Y.; Deng, L.; Li, J.; Guo, S.; Wang, E.; Dong, S. *ACS Nano* **2011**, *5*, 1282−1290.

(3) Manohar, S.; Mantz, A. R.; Bancroft, K. E.; Hui, C.-Y.; Jagota, A.; Vezenov, D. V. *Nano Lett.* **2008**, *8*, 4365−4372.

(4) Varghese, N.; Mogera, U.; Govindaraj, A.; Das, A.; Maiti, P. K.; Sood, A. K.; Rao, C. N. R. *ChemPhysChem* **2009**, *10*, 206−210.

(5) Park, J. S.; Na, H.-K.; Min, D.-H.; Kim, D.-E. *Analyst* **2013**, *138*, 1745−1749.

(6) Huang, P.-J. J.; Liu, J. *Anal. Chem.* **2012**, *84*, 4192−4198.

(7) Tang, L.; Chang, H.; Liu, Y.; Li, J. *Adv. Funct. Mater.* **2012**, *22*, 3083−3088.

(8) (a) Li, F.; Huang, Y.; Yang, Q.; Zhong, Z. T.; Li, D.; Wang, L. H.; Song, S. P.; Fan, C. H. *Nanoscale* **2010**, *2*, 1021−1026. (b) Dong, H. F.; Gao, W. C.; Yan, F.; Ji, H. X.; Ju, H. X. *Anal. Chem.* **2010**, *82*, 5511−5517. (c) Guo, Y.; Deng, L.; Li, J.; Guo, S.; Wang, E.; Dong, S. *ACS Nano* **2011**, *5*, 1282−1290. (d) Wu, W.; Hu, H.; Li, F.; Wang, L.; Gao, J.; Lu, J.; Fan, C. *Chem. Commun.* **2011**, *47*, 1201−1203. (e) Song, Z.-L.; Zhao, X.-H.; Liu, W.-N.; Ding, D.; Bian, X.; Liang, H.; Zhang, X.-B.; Chen, Z.; Tan, W. *Small* **2012**, *9*, 951−957.

(9) Wen, Y. Q.; Xing, F. F.; He, S. J.; Song, S. P.; Wang, L. H.; Long, Y. T.; Li, D.; Fan, C. H. *Chem. Commun.* **2010**, *46*, 2596−2598.

(10) Song, Y. J.; Qu, K. G.; Zhao, C.; Ren, J. S.; Qu, X. G. *Adv. Mater.* **2010**, *22*, 2206−2210.

(11) Wang, Y.; Li, Z. H.; Hu, D. H.; Lin, C. T.; Li, J. H.; Lin, Y. H. *J. Am. Chem. Soc.* **2010**, *132*, 9274−9276.

(12) Lu, C.-H.; Li, J.; Lin, M.-H.; Wang, Y.-W.; Yang, H.-H.; Chen, X.; Chen, G.-N. *Angew. Chem., Int. Ed.* **2010**, *49*, 8454−8457.

(13) Tan, X.; Chen, T.; Xiong, X.; Mao, Y.; Zhu, G.; Yasun, E.; Li, C.; Zhu, Z.; Tan, W. *Anal. Chem.* **2012**, *84*, 8622−8627.

(14) Chang, H. X.; Tang, L. H.; Wang, Y.; Jiang, J. H.; Li, J. H. *Anal. Chem.* **2010**, *82*, 2341−2346.

(15) Wang, L.; Pu, K.-Y.; Li, J.; Qi, X.; Li, H.; Zhang, H.; Fan, C.; Liu, B. *Adv. Mater.* **2011**, *23*, 4386−4391.

(16) Cheng, C.-L.; Zhao, G.-J. *Nanoscale* **2012**, *4*, 2301−2305.

(17) Akdim, B.; Pachter, R.; Day, P. N.; Kim, S. S.; Naik, R. R. *Nanotechnology* **2012**, *23*, 165703.

(18) Iliafar, S.; Wagner, K.; Manohar, S.; Jagota, A.; Vezenov, D. *J. Phys. Chem. C* **2012**, *116*, 13896−13903.

(19) Gowtham, S.; Scheicher, R. H.; Ahuja, R.; Pandey, R.; Karna, S. P. *Phys. Rev. B* **2007**, *76*, 033401.

(20) Gomez-Navarro, C.; Meyer, J. C.; Sundaram, R. S.; Chuvilin, A.; Kurasch, S.; Burghard, M.; Kern, K.; Kaiser, U. *Nano Lett.* **2010**, *10*, 1144−1148.

(21) Erickson, K.; Erni, R.; Lee, Z.; Alem, N.; Gannett, W.; Zettl, A. *Adv. Mater.* **2010**, *22*, 4467−4472.

(22) Lu, C. F.; Nadarajah, A.; Chittur, K. K. *J. Colloid Interface Sci.* **1994**, *168*, 152−161.

(23) Hall, D. *Anal. Biochem.* **2001**, *288*, 109−125.

(24) Wang, K. M.; Tang, Z. W.; Yang, C. Y. J.; Kim, Y. M.; Fang, X. H.; Li, W.; Wu, Y. R.; Medley, C. D.; Cao, Z. H.; Li, J.; Colon, P.; Lin, H.; Tan, W. H. *Angew. Chem., Int. Ed.* **2009**, *48*, 856−870.

(25) Vallee-Belisle, A.; Ricci, F.; Plaxco, K. W. *J. Am. Chem. Soc.* **2012**, *134*, 2876−2879.

(26) Ricci, F.; Vallee-Belisle, A.; Porchetta, A.; Plaxco, K. W. *J. Am. Chem. Soc.* **2012**, *134*, 15177−15180.
(27) Lu, C. H.; Li, J.; Liu, J. J.; Yang, H. H.; Chen, X.; Chen, G. N. *Chem.—Eur. J.* **2010**, *16*, 4889−4894.
(28) Zhou, J.; Lu, Q.; Tong, Y.; Wei, W.; Liu, S. *Talanta* **2012**, *99*, 625−630.
(29) (a) Yang, R. H.; Jin, J. Y.; Chen, Y.; Shao, N.; Kang, H. Z.; Xiao, Z.; Tang, Z. W.; Wu, Y. R.; Zhu, Z.; Tan, W. H. *J. Am. Chem. Soc.* **2008**, *130*, 8351−8358. (b) Zhu, C.; Zeng, Z.; Li, H.; Li, F.; Fan, C.; Zhang, H. *J. Am. Chem. Soc.* **2013**, *135*, 5998−6001. (c) Opdahl, A.; Petrovykh, D. Y.; Kimura-Suda, H.; Tarlov, M. J.; Whitman, L. J. *Proc. Natl. Acad. Sci. U.S.A.* **2007**, *104*, 9−14. (d) Schreiner, S. M.; Shudy, D. F.; Hatch, A. L.; Opdahl, A.; Whitman, L. J.; Petrovykh, D. Y. *Anal. Chem.* **2010**, *82*, 2803−2810. (e) Li, H.; Zhang, Y.; Wang, L.; Tian, J.; Sun, X. *Chem. Comm* **2011**, *47*, 961−963. (f) Li, H.; Zhang, Y.; Luo, Y.; Sun, X. *Small* **2011**, *7*, 1562−1568. (g) Zhai, J.; Li, H.; Sun, X. *RSC Adv.* **2011**, *1*, 36−39. (h) Yang, R. H.; Tang, Z. W.; Yan, J. L.; Kang, H. Z.; Kim, Y. M.; Zhu, Z.; Tan, W. H. *Anal. Chem.* **2008**, *80*, 7408−7413.